

ABSTRACT: To determine the degree to which intramuscular pressure (IMP) and muscle force are correlated in an intact compartment, a custom pressure transducer was inserted into the rabbit tibialis anterior (TA) while activating the muscle via the peroneal nerve and measuring TA muscle force distal to the ankle retinaculum. In general, IMP was more variable compared with muscle force throughout the entire isometric length–tension relationship. In contrast to results obtained on isolated TA muscles, IMP–force relations with the compartment intact were not significantly different between the ascending and descending limbs of the length–tension curve. Specifically, average relative pressure–force coefficients of determination (r^2) were 0.76 ± 0.11 for the active ascending limb and 0.98 ± 0.01 for the active descending limb. These data demonstrate that muscle force and IMP are fairly well correlated under isometric conditions and that this relationship is not improved by measuring IMP in an intact environment.

Muscle Nerve 40: 79–85, 2009

CORRELATION BETWEEN ISOMETRIC FORCE AND INTRAMUSCULAR PRESSURE IN RABBIT TIBIALIS ANTERIOR MUSCLE WITH AN INTACT ANTERIOR COMPARTMENT

TAYLOR M. WINTERS, MS,¹ GENARO S. SEPULVEDA, BS,¹ PATRICK S. COTTLER, PhD,² KENTON R. KAUFMAN, PhD,³ RICHARD L. LIEBER, PhD,^{1,4} and SAMUEL R. WARD, PT, PhD^{1,4,5}

¹ Department of Bioengineering, University of California San Diego, San Diego, California, USA

² Luna Innovations, Charlottesville, Virginia, USA

³ Department of Orthopedics, Mayo Clinic, Rochester, Minnesota, USA

⁴ Department of Orthopedic Surgery, University of California, San Diego and Veterans Administration Medical Center, 9500 Gilman Avenue MC 9151, San Diego, California 92023, USA

⁵ Department of Radiology, University of California San Diego, San Diego, California, USA

Accepted 8 January 2009

Human skeletal muscle functional studies are notable for the variety of methodological approaches used. Functional evaluation of human muscle may range in scale from the highly invasive direct measurement of active^{8,18} or passive¹³ muscle force to non-invasive or minimally invasive inference of function based on the electromyogram (EMG^{9,23}) or a muscle image (ultrasound^{3,15} and magnetic resonance imaging^{12,25}). For the purposes of assigning cause–effect relationships between muscle function

and individual performance, it is desirable to obtain direct muscle function measurements in a clinically acceptable manner.

The most promising approach for obtaining such unambiguous information (absent modeling assumptions) is direct measurement of intramuscular pressure (IMP) during voluntary movement. Muscle IMP measurements have had great popularity in the clinical and applied physiological literature where descriptive studies have correlated IMP with ground reaction force,² isometric joint torque,²⁶ and the onset of compartment syndrome.¹¹ In these situations, it has been assumed that IMP serves as an accurate surrogate of muscle force. Yet only recently has IMP been directly compared with muscle force.⁶ In that study, it was found that muscle force and IMP were reasonably correlated but that the IMP measurements were much more variable than force measurements, with coefficients of variations approaching 100%. However, this study was performed with the anterior compartment muscles of the leg exposed. IMP has been shown previously in clinical

Abbreviations: EMG, electromyogram; ICC, intraclass correlation coefficient; IMP, intramuscular pressure; l_0 , peak intramuscular pressure; L_m , literature optimal muscle length for the tibialis anterior; L_o , experimentally measured optimal muscle length for the tibialis anterior; P_o , peak tension; PCSA, physiological cross-sectional area; r^2 , coefficient of determination; TA, tibialis anterior

Key words: fluid mechanics; fluid pressure; intramuscular pressure; isometric contraction; length–tension relationship

Disclosure: P.C. is employed by Luna Innovations, the manufacturer of the pressure transducer

Correspondence to: S.R. Ward; e-mail: snward@ucsd.edu

© 2009 Wiley Periodicals, Inc.

Published online 15 June 2009 in Wiley InterScience (www.interscience.wiley.com). DOI 10.1002/mus.21298

and cadaveric studies to correlate with tissue depth and muscle position,¹⁰ and with transducer movement in basic science studies.²⁸

We suspected that retaining the myofascial boundaries may help anchor the transducer and minimize transducer movement, thereby improving the muscle stress–IMP correlation. The importance of this approach is to design an experiment that reflects the clinical use of the device, because one of the intended applications of IMP measurement in humans is to understand movement and aid in the surgical decision-making process.^{5,27} Thus, the purpose of this study was to measure the muscle force–IMP correlation under conditions of intact skin and fascia to quantify the degree to which IMP serves as a surrogate for active and passive force.

METHODS

Experiments performed in this investigation were similar to previously described methods,⁶ but the anterior compartment of the leg remained intact. The tibialis anterior (TA) muscle from the New Zealand white rabbit (mass 2.6 ± 0.3 kg; $n = 9$) was chosen for force and pressure measurements based on its accessibility, parallel fiber arrangement (pennation angle of 3° ²⁰), and predominantly fast-fiber-type percentage (95% fast fibers^{1,19,24}). Control experiments demonstrated that the small transducer tip, representing only 0.2% of the muscle's physiological cross-sectional area (PCSA),⁶ did not affect isometric force production after 40 isometric contractions. The protocol was approved by the Department of Veterans Affairs, San Diego Committee on the Use of Animal Subjects in Research. All experimental procedures were performed in accordance with the guidelines set forth by the *Guide for the Care and Use of Animals* (National Institutes of Health).

Animal preparation and measurement of isometric contractile properties were performed essentially as described previously,^{21,22} but they were modified to ensure that the anterior compartment remained intact. Briefly, rabbits were anesthetized with 5% isoflurane and a subcutaneous injection of a ketamine–xylazine cocktail (50 and 5 mg/kg body mass, respectively) and maintained on 2% isoflurane anesthesia. Heart rate and oxygen saturation were monitored (VetOx; Heska Co., Fort Collins, Colorado) throughout the test, and anesthesia level was adjusted as needed. Two-centimeter incisions made at the medial and lateral femoral condyles and just proximal to the medial and lateral malleoli of the leg allowed 3.2-mm Steinmann pins to be drilled through the femur and tibia. The pins were used to

secure the leg to a custom-made jig for muscle testing. The lateral femoral condyle incision was extended, and the biceps femoris was split to expose the peroneal nerve. A cuff electrode was placed around the peroneal nerve for direct muscle activation (Pulsar 6Bp Stimulator; FHC, Bowdoinham, Maine). A fifth incision was made distal to the extensor retinaculum. The distal TA tendon was transected and clamped to a servo-motor (Cambridge Model 310B; Aurora Scientific, Aurora, Ontario, Canada), which controls muscle length and measures force. It was located at the muscle–tendon junction, and it was aligned with the force-generating axis of the motor (Fig. 1). Muscle temperature was maintained at 37°C with radiant heat, mineral oil, and a servo-temperature controller (Model 73A; YSI, Yellow Springs, Ohio). A $250\text{-}\mu\text{m}$ -diameter fiber-optic pressure sensor (Luna Innovations, Blacksburg, Virginia) was inserted via a 20-gauge angiocatheter needle at approximately 10° in the sagittal plane in line with the force-generating axis of the fibers in the midbelly of the muscle (Fig. 2). The pressure performance characteristics of the force transducer¹⁶ showed a mean accuracy of $1.45 \pm 0.32\%$ and a mean repeatability of $1.5 \pm 0.81\%$ (five different transducers tested in vitro).

The length–tension protocol consisted of a series of 100 Hz tetanic contractions (pulse width 0.3 ms, amplitude 10 V) over a 640-ms period. Two-minute rest intervals were interposed between contractions to minimize fatigue effects. Measurements began at a zeroed motor length and ranged from -30% muscle length (L_m) to $30\% L_m$ in increments of $5\% L_m$. L_m was assumed to be 56.84 mm—the literature optimal muscle length for the TA.²⁰ This length was chosen, because muscle length could not be measured directly with the compartment intact. Passive muscle force was defined as the resting muscle force at each length and measured for each contraction bout during the 100-ms period prior to muscle stimulation. Length, force, and pressure were recorded for each contraction using a data acquisition board (610E series; National Instruments, Austin, Texas) and a custom-written LabVIEW program (National Instruments) acquiring data at 4 kHz per channel.

Upon completion of testing, animals were euthanized with pentobarbital (Euthasol; Virbac AH, Fort Worth, Texas). The skin and fascia surrounding the TA were excised to validate the position of the intramuscular pressure sensor, and the sensor was gently removed. The muscle was pinned to a corkboard at a length of ≈ 56 mm and fixed in 10% phosphate-buffered formalin for 48 hours. After rinsing in isotonic phosphate-buffered saline and digestion in

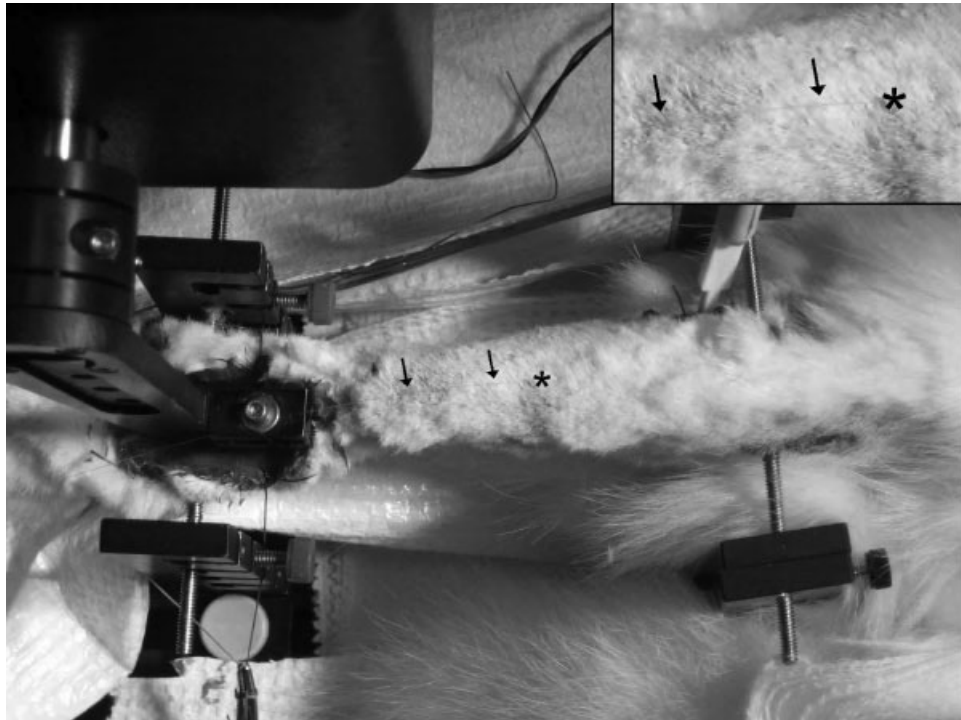


FIGURE 1. Experimental apparatus used to measure isometric force–intramuscular pressure relationship with an intact anterior compartment. The rabbit hindlimb is immobilized in a custom jig via Steinmann pins securing the distal femur and ankle joint. A cuff electrode is placed around the peroneal nerve to activate the TA. Arrows mark the path of the pressure sensor with the star depicting the insertion position. Inset: Close-up view of the pressure sensor insertion.

15% H_2SO_4 for 20 minutes, three muscle fiber bundles were microdissected from the proximal, middle, and distal regions of the muscle to yield representative sarcomere lengths (L_s) across the entire muscle. Fiber bundle length was measured under a dissecting microscope to the nearest micron from two different fiber bundles in each of the three regions, providing six measurements of bundle length across

the entire muscle. The L_s of each bundle was measured by laser diffraction in three regions of each muscle; thus, the whole-muscle sarcomere length was calculated as the average of 18 L_s measurements obtained from the entire muscle. This permitted muscle length normalization to a sarcomere length of $2.27 \mu\text{m}$,⁴ yielding an experimentally measured optimal muscle length (L_o) for each animal.⁷

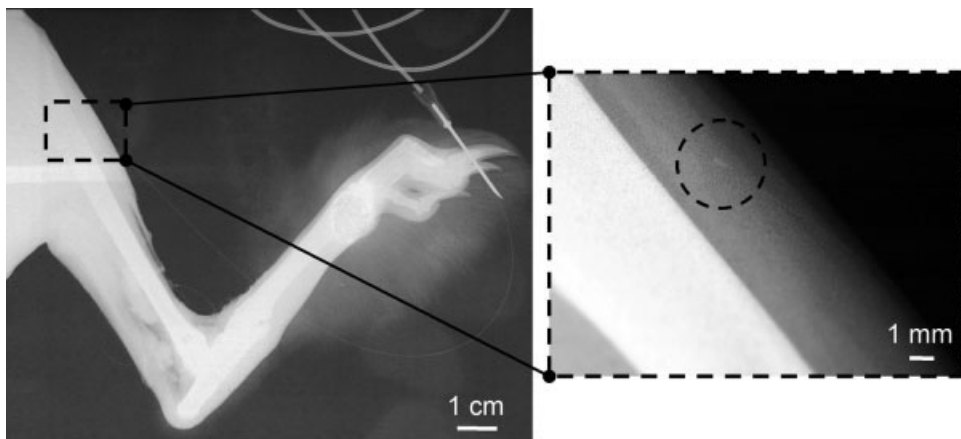


FIGURE 2. Lateral X-ray of the rabbit hindlimb with sensor. Left: Placement of the sensor in the mid-belly of the TA muscle. Right: Sensor tip placed mid-muscle with approximately 5 mm of the sensor entering the muscle.

Active and passive force and IMP records were converted to relative tension and relative IMP by dividing by peak force (P_o) and peak IMP (I_o), respectively, for the purpose of comparing the two measurements. The experimentally measured absolute muscle lengths were divided by the animal-specific normalized muscle lengths (L_o) to obtain relative muscle lengths. Because L_o was not determined until experiments were completed, relative lengths were not identical among trials. Thus, active data were fit with a second-order polynomial (force: $r^2 = 0.93 \pm 0.02$; IMP: $r^2 = 0.70 \pm 0.07$), and passive data were fitted with a third-order polynomial (force: $r^2 = 0.95 \pm 0.02$; IMP: $r^2 = 0.81 \pm 0.05$), to facilitate interpolation in 5% muscle length increments. To characterize the relative agreement between the relative tension and relative IMP data, the coefficient of determination (r^2) was quantified using SPSS statistical software (SPSS, Inc., Chicago, Illinois). Likewise, the intraclass correlation coefficient (ICC) was employed to quantify absolute agreement between the data sets. The r^2 and ICC values were calculated for the ascending limb (defined as lengths less than or equal to L_o), the descending limb (defined as lengths greater than L_o), and both limbs (all data) for the purpose of examining the underlying contributions of each limb to the active IMP signal. In investigating the passive IMP signal, relative tension and IMP data for the entire curve were analyzed. Differences in ascending and descending limbs and differences in active and passive relationships were compared with paired t -tests. All data are presented as mean \pm SEM unless otherwise stated. Significance was set to $P < 0.05$ and presented as a range when depicting significance across trials.

RESULTS

The raw intramuscular pressure–time traces mimicked the general shape of the raw isometric force–time traces, but they exhibited a drop in pressure over the course of activation (Fig. 3) as previously reported.⁶ As expected, the muscle length–isometric tension curve was characterized by an ascending limb at lengths less than L_o and a descending limb with passive tension rising exponentially at lengths greater than L_o (Fig. 4A). Stress at optimal length was 298.2 ± 3.7 kPa. Similarly, the length–intramuscular pressure relationship was also characterized by an ascending and descending limb for most individual trials (Fig. 4B), despite the difference in length at which optimal force and pressure occurred. This yielded high variability and an irregular shape of the length–intramuscular pressure relationship in com-

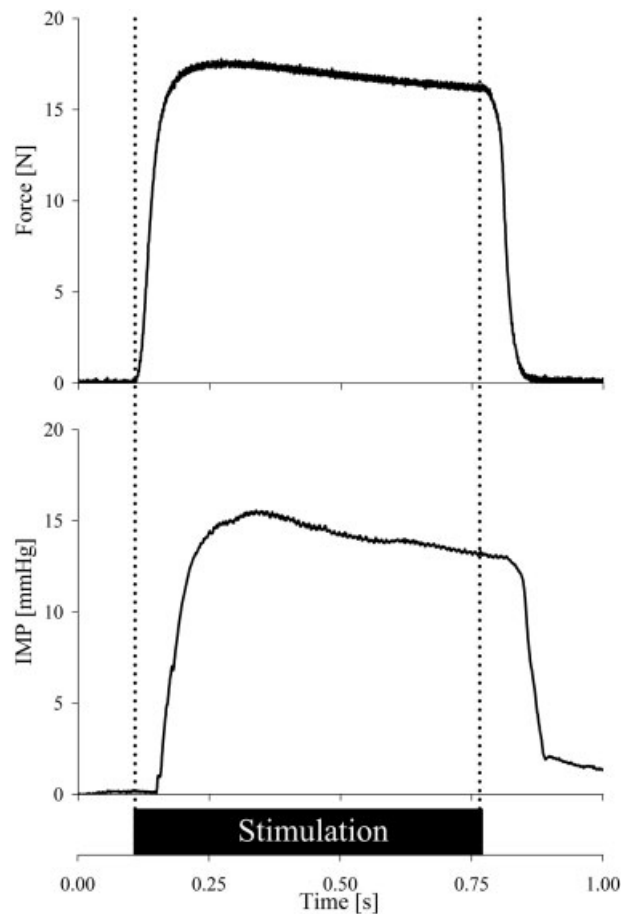


FIGURE 3. Sample record of muscle force (N) and intramuscular pressure (mm Hg) recordings from an isometric contraction. Average force and intramuscular pressure values on the plateau were used to construct the length–tension and length–IMP relations. The period of muscle activation is denoted by the solid bar at the bottom and vertical dotted lines.

parison to tension. As seen previously,⁶ pressure declined more rapidly than tension at long lengths. The passive relative pressure curve had a similar shape to the passive relative tension, and it also had a higher degree of variability.

A positive linear correlation was found between relative tension and relative intramuscular pressure for both the ascending and descending limbs (Table 1). Relative pressure–force coefficient of determination (r^2) averaged 0.76 ± 0.11 ($P < 0.001$ – 0.114) for the active ascending limb and 0.98 ± 0.01 ($P < 0.001$) for the active descending limb. The passive coefficient of determination averaged 0.77 ± 0.05 ($P < 0.001$ – 0.003) for both limbs combined. In contrast to our previous report on the isolated TA,⁶ pressure–stress correlations for the ascending limb of the length–tension curve and descending limb were not significantly different ($P = 0.091$). How-

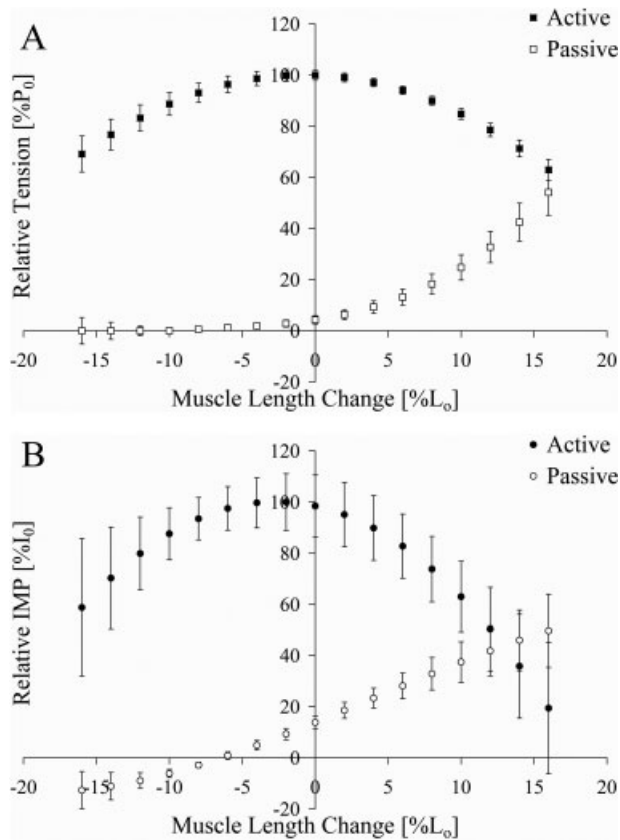


FIGURE 4. Relationship between relative change in length and **(A)** average isometric force or **(B)** average intramuscular pressure for the rabbit tibialis anterior. Filled symbols represent measurements from activated muscles, whereas open symbols represent measurements from passive muscles. Force and pressure correlations did not differ between limbs, and passive stretch generally maintained higher correlations (see Table 1 for details). Data are plotted as mean \pm SEM.

ever, correlations for active tension ($r^2 = 0.61 \pm 0.13$) were generally lower than those for passive tension ($r^2 = 0.77 \pm 0.05$). An overall significant absolute agreement was found between intramuscular pressure and tension. Average ICC value was 0.60 ± 0.11 ($P < 0.001$ – 0.946) for the active ascend-

ing limb and 0.49 ± 0.11 ($P < 0.001$ – 0.275) for the active descending limb. The passive pressure–tension relation yielded an ICC of 0.80 ± 0.03 ($P < 0.001$ – 0.034).

Linear regression of relative tension and intramuscular pressure yielded a slope of 1.57 ± 0.22 with an intercept of -63.91 ± 28.13 . Decomposing this into ascending and descending limbs resulted in slopes of 1.48 ± 0.28 and 1.58 ± 0.31 , respectively, which were not significantly different from each other ($P = 0.827$). Intercepts were also not significantly different ($P = 0.906$), with values of -87.18 ± 52.57 and -93.32 ± 30.57 for the ascending and descending limbs, respectively. The passive tension–IMP regression yielded a slope of 0.94 ± 0.07 and intercept of 6.72 ± 1.70 . A comparison of the active and passive regressions resulted in a significant difference between both the slope ($P = 0.042$) and intercept ($P = 0.034$).

DISCUSSION

The purpose of this study was to define the relationship between isometric force generation and intramuscular pressure (IMP) under conditions in which the myofascial compartment was intact. Our main finding was that the previous demonstration of good correlations between these two parameters remained true but did not improve in spite of the compartment remaining intact. These data suggest that continuity of the myofascial compartment does not change the IMP–force relationship observed in isolated muscle systems. Thus, these data provide support for the ability of IMP to predict muscle force in a clinical setting.

In contrast to previous studies, no differences between the pressure–force correlations were observed on the ascending compared with the descending limb of the length–tension curve. Previously, based on a higher correlation observed between pressure and force on the descending limb, we hy-

Table 1. Summary of relative isometric tension–pressure correlations.*

Activation state	Limb of the length–tension curve	Coefficient of determination (r^2)		Intraclass correlation coefficient (ICC)	
		Mean \pm SEM	Range (min–max)	Mean \pm SEM	Range (min–max)
Active	Ascending limb	0.76 ± 0.11	0.16–0.99	0.60 ± 0.11	0.16–0.99
	Descending limb	0.98 ± 0.01	0.90–0.99	0.49 ± 0.11	0.09–0.99
	Ascending + descending limb	0.61 ± 0.13	0.10–0.99	0.48 ± 0.12	0.18–0.99
Passive	Ascending + descending limb	0.77 ± 0.05	0.51–0.93	0.80 ± 0.03	0.66–0.93

*Values represent mean \pm standard error for 9 animals.

pothesized that, at longer lengths, the pressure transducer was held more securely in the muscle tissue, thus minimizing movement artifact.⁶ Indeed, direct high-speed video recordings of muscle contractions subsequently demonstrated the critical effect of transducer movement on the fidelity of the pressure signal. When transducer movement occurred, the pressure curve was almost completely dissociated from the force curve, even after transducer movement ceased.²⁸ Based on this finding, we suspected that an intact myofascial compartment might secure the transducer more firmly, as compared with the case of an isolated muscle, and improve the pressure–force correlation. However, this was not the case.

Previous studies of intramuscular pressure have described factors that affect the magnitude of measured pressure. For example, depth, proximity to bone, and muscle curvature have been isolated as important factors that define absolute muscle pressure levels.^{10,26} In several pilot studies in which multiple pressure transducers were inserted into a single muscle, we found qualitative and quantitative differences among the absolute pressure records recorded. It thus appears that the pressure records obtained herein may represent a relatively local phenomenon.

The data may provide some insights into the mechanism of pressure generation in skeletal muscle. Specifically, we observed that IMP declines more rapidly than active force as muscle length increases on the descending limb (Fig. 4). This observation is consistent with the idea that contractions at longer lengths may disrupt parallel passive structures in the tissue, such as connective tissue, intermediate filament meshes, and even muscle cell–extracellular matrix interactions.¹⁷ If disruption occurs, it might be expected that the muscle contractile force would be dissipated throughout the tissue, and the pressure rise would not scale directly with myofibril overlap. Of course, this assertion must be tested experimentally. Because finite-element models have suggested that muscle tissue strain and pressure are causally related,¹⁴ the data suggest that muscle strains are not dramatically affected by superficial fascia and skin.

In conclusion, these experiments demonstrate that IMP and muscle force are roughly correlated in both the passive and active conditions. This correlation is not superior to that observed for the isolated TA, suggesting that anterior compartment patency does not affect the fundamental nature of pressure generation in skeletal muscle.

This study was supported by Grant HD31476 from the Department Veterans Affairs and NIH/NICHHD. The authors thank Shannon Bremner for her expertise in the development of the LabVIEW program. We honor the memory of Dr. David Sutherland for inspiring this line of research and providing the fertile environment for inquiry at the Children’s Hospital of San Diego.

REFERENCES

1. Aigner S, Gohlsch B, Hamalainen N, Staron RS, Uber A, Wehrle U, et al. Fast myosin heavy chain diversity in skeletal muscles of the rabbit: heavy chain II_d, not II_b predominates. *Eur J Biochem* 1993;211:367–372.
2. Ballard RE, Watenpaugh DE, Breit GA, Murthy G, Holley DC, Hargens AR. Leg intramuscular pressures during locomotion in humans. *J Appl Physiol* 1998;84:1976–1981.
3. Braekken IH, Majida M, Ellstrom-Eng M, Dietz HP, Umek W, Bo K. Test–retest and intra-observer repeatability of two-, three- and four-dimensional perineal ultrasound of pelvic floor muscle anatomy and function. *Int Urogynecol J Pelvic Floor Dysfunct* 2008;19:227–235.
4. Burkholder TJ, Lieber RL. Sarcomere length operating range of vertebrate muscles during movement. *J Exp Biol* 2001;204:1529–1536.
5. Chambers H, Lauer A, Kaufman K, Cardelia JM, Sutherland D. Prediction of outcome after rectus femoris surgery in cerebral palsy: the role of cocontraction of the rectus femoris and vastus lateralis. *J Pediatr Orthop* 1998;18:703–711.
6. Davis J, Kaufman KR, Lieber RL. Correlation between active and passive isometric force and intramuscular pressure in the isolated rabbit tibialis anterior muscle. *J Biomech* 2003;36:505–512.
7. Felder A, Ward SR, Lieber RL. Sarcomere length measurement permits high resolution normalization of muscle fiber length in architectural studies. *J Exp Biol* 2005;208:3275–3279.
8. Gregor RJ, Komi PV, Browning RC, Jarvinen M. A comparison of the triceps surae and residual muscle moments at the ankle during cycling. *J Biomech* 1991;24:287–297.
9. Hallen LG, Lindahl O. Muscle function in knee extension. An EMG study. *Acta Orthopaed Scand* 1967;38:434–444.
10. Hargens AR, Akeson WH, Mubarak SJ, Owen CA, Gershuni DH, Garfin SR, et al. Kappa Delta Award paper. Tissue fluid pressures: from basic research tools to clinical applications. *J Orthop Res* 1989;7:902–909.
11. Hargens AR, Mubarak SJ. Current concepts in the pathophysiology, evaluation, and diagnosis of compartment syndrome. *Hand Clinics* 1998;14:371–383.
12. Hides J, Wilson S, Stanton W, McMahon S, Keto H, McMahon K, et al. An MRI investigation into the function of the transversus abdominis muscle during “drawing-in” of the abdominal wall. *Spine* 2006;31:E175–E178.
13. Hoang PD, Herbert RD, Todd G, Gorman RB, Gandevia SC. Passive mechanical properties of human gastrocnemius muscle tendon units, muscle fascicles and tendons in vivo. *J Exp Biol* 2007;210:4159–4168.
14. Jenkyn TR, Koopman B, Huijing P, Lieber RL, Kaufman KR. Finite element model of intramuscular pressure during isometric contraction of skeletal muscle. *Phys Med Biol* 2002;47:4043–4061.
15. Johnson JH, Amend JF, Franklin D, Garner HE. Measurement of specific laryngeal muscle function by ultrasound. *Arch Oto-Rhino-Laryngol* 1978;220:225–229.
16. Kaufman KR, Wavering T, Morrow D, Davis J, Lieber RL. Performance characteristics of a pressure microsensor. *J Biomech* 2003;36:283–287.
17. Kjaer M. Role of extracellular matrix in adaptation of tendon and skeletal muscle to mechanical loading. *Physiol Rev* 2004;84:649–698.

18. Komi PV, Fukashiro S, Jarvinen M. Biomechanical loading of Achilles tendon during normal locomotion. *Clin Sports Med* 1992;11:521–531.
19. Lexell J, Jarvis JC, Currie J, Downham DY, Salmons S. Fibre type composition of rabbit tibialis anterior and extensor digitorum longus muscles. *J Anat* 1994;185:95–101.
20. Lieber RL, Blevins FT. Skeletal muscle architecture of the rabbit hindlimb: functional implications of muscle design. *J Morphol* 1989;199:93–101.
21. Lieber RL, Fridén J. Muscle damage is not a function of muscle force but active muscle strain. *J Appl Physiol* 1993;74:520–526.
22. Lieber RL, Woodburn TM, Fridén J. Muscle damage induced by eccentric contractions of 25% strain. *J Appl Physiol* 1991;70:2498–2507.
23. Meurer A, Bodem F, Heine J. Ensemble averaging and multiple statistical testing of EMG activities of cyclically repeated body motions. A tool for muscle function analysis in experimental and clinical orthopaedics. *Biomed Technik* 2003;48:235–240.
24. Peter JB, Barnard RJ, Edgerton VR, Gillespie CA, Stempel KE. Metabolic profiles of three fiber types of skeletal muscle in guinea pigs and rabbits. *Biochemistry* 1972;11:2627–2633.
25. Prompers JJ, Jeneson JA, Drost MR, Oomens CC, Strijkers GJ, Nicolay K. Dynamic MRS and MRI of skeletal muscle function and biomechanics. *NMR Biomed* 2006;19:927–953.
26. Styf J, Ballard R, Aratow M, Crenshaw A, Watenpaugh D, Hargens AR. Intramuscular pressure and torque during isometric, concentric and eccentric muscular activity. *Scand J Med Sci Sports* 1995;5:291–296.
27. Sutherland DH, Zilberfarb JL, Kaufman KR, Wyatt MP, Chambers HG. Psoas release at the pelvic brim in ambulatory patients with cerebral palsy: operative technique and functional outcome. *J Pediatr Orthop* 1997;17:563–570.
28. Ward SR, Davis J, Kaufman KR, Lieber RL. Relationship between muscle stress and intramuscular pressure during dynamic muscle contractions. *Muscle Nerve* 2007;36:313–319.